UHPFRC failure analysis using a geometrically exact Extended Lumped Damage Mechanics approach

Daniel V. C. Teles[1], David L. N. F. Amorim[1,2,3], Edson D. Leonel[1]

[1]*Graduate Program of Civil Engineering, São Carlos School of Engineering, University of São Paulo*
Av. Trabalhador são-carlense 400, Pq. Arnold Schimidt, São Carlos, 13566-590, São Paulo, Brazil
danielvcteles@usp.br, davidnf@academico.ufs.br, edleonel@sc.usp.br
[2]*Disaster Research Institute, Federal University of Sergipe*
Av. Marcelo Deda Chagas s/n, Rosa Elze, São Cristóvão, 49107-230, Sergipe, Brazil
davidnf@academico.ufs.br
[3]*Graduate Program of Civil Engineering, Federal University of Alagoas*
Av. Lourival Melo Mota s/n, Tabuleiro do Martins, Maceió, 57072-970, Alagoas, Brazil
davidnf@academico.ufs.br

Abstract. The use of ultra-high-performance fibre-reinforced concrete (UHPFRC) has significantly increased in the recent years. However, the accurate mechanical behaviour modelling of this complex material is still a challenge in the present. Due to the materials high load-bearing capacity and the presence of fibres, this type of problem experiments large displacements before the failure. In this study, the material damage description has been performed by the Extended Lumped Damage Mechanics. Additionally, an approach based on the nodal positions of the Finite Element Method has been utilised, which makes the formulation geometrically exact. Thus, this study evaluates the failure of structures composed of UHPFRC, accounting for the effects of material and geometric nonlinearities handled by the Extended Lumped Damage Mechanics and the Finite Element Method based on positions, respectively.

Keywords: Ultra-high-performance fibre-reinforced concrete, lumped damage mechanics, finite element based on positions

1 Introduction

The use of ultra-high-performance concrete (UHPC) has significantly increased in recent years. Particularly due to the wide application of slender structures and the development of materials with superior mechanical properties. This material, which tends to fail in a brittle manner, can have its mechanical characteristics improved by adding fibres (UHPFRC). The manufacture of this type of material presents high costs, making it difficult to perform large-scale experimental analyses, which justifies the development of numerical tools for parametric studies of structures composed of UHPFRC.

The finite element method (FEM) is one of the most used numerical methods for structural analysis. By discretizing the domain and adopting approximating functions, nodal responses can be obtained for the problem. Recently, a position-based approach was proposed by Coda and Greco [1] to analyze planar frames. In this approach, named as positional FEM, the equilibrium is performed as a function of the nodal position considering the current problem configuration, which allows the formulation of geometrically exact finite elements. Subsequently, the approach has been used in several problems, such as spatial trusses [2], solid domains (plates and shells) [3, 4], fluid-structure iteration [5], solids composed of viscoelastic materials [6] and study of structural instability [7].

To model the mechanical behaviour of composite materials, Vanalli et al. [8] presented a technique that allows the representation of fibres with perfect adhesion using the FEM. The proposed approach does not add degrees of freedom to the problem, making it computationally efficient. In addition, the nodes of the element used to discretise the fibres do not need to coincide with those used to discretise the solid, facilitating mesh generation. Subsequently, Sampaio et al. [9] extended the technique to the position-based formulation.

Lumped damage mechanics (LDM) emerged as a simplified alternative to consider material nonlinearity in frames [10]. The approach uses concepts of fracture mechanics and classical damage applied to plastic hinges from plasticity theory. Subsequently, the theory has been extended to enable the analysis of different complex

engineering problems, such as seismic analyses in frames [11–13], analysis of beams and simple concrete tunnels [14], reinforced concrete arches [15, 16], metallic frames [17, 18], beams subjected to impact loads [19, 20], corrosion [21], concrete tunnel segments with fibres [22] and collapse mechanisms for RC frames subjected to earthquakes [23]. The expansion of the approach to the analysis of two-dimensional solids (Extended Lumped Damage Mechanics) has been successful [24, 25], including the description of the experimental behaviour of common engineering materials [26].

Thus, the present study evaluates the failure of structures composed of UHPFRC, considering the effects of material and geometric nonlinearities handled by the Extended Lumped Damage Mechanics (XLDM) and the Finite Element Method based on positions, respectively.

2 Finite element method based on positions

The main characteristic of the approach involves the equilibrium description as a function of the nodal positions in the current configuration of the problem. By the principle of stationarity, the equilibrium condition is reached when the first variation of the total mechanical energy Π is zero. Thus, considering static problems, where $\mathbb{U}$ is internal energy and $\mathbb{P}$ the potential of external loads, the equilibrium condition is:

$$\frac{\partial \Pi}{\partial Y_i} = \frac{\partial \mathbb{U}}{\partial Y_i} + \frac{\partial \mathbb{P}}{\partial Y_i} = F_i^{int} - F_i^{ext} = 0_i \tag{1}$$

where Y_i is the current nodal position, F_i^{int} is the internal force and F_i^{ext} is the external force.

As the equilibrium presented in equation 1 is nonlinear, the system is solved iteratively by the Newton-Raphson method, with the correction of the nodal positions calculated from:

$$r_i(Y) = r_i(Y^0) + \left.\frac{\partial r_i}{\partial Y_k}\right|_{Y^0} \Delta Y_k = 0_i \Rightarrow \Delta Y_k = -\left(\left.\frac{\partial r_i}{\partial Y_k}\right|_{Y^0}\right)^{-1} r_i(Y^0) \tag{2}$$

where r_i is the mechanical non-equilibrated vector (or residual vector), Y^0 is the tentative nodal position, Y is the current nodal position (solution of the system), and ΔY_k is the nodal position correction.

In the case of conservative external forces, the tangent stiffness matrix is as follows:

$$\left.\frac{\partial r_i}{\partial Y_k}\right|_{Y^0} = \left.\frac{\partial^2 \mathbb{U}}{\partial Y_k \partial Y_i}\right|_{Y^0} \tag{3}$$

In addition, in the part referring to the internal energy, the Saint Venant-Kirchhoff (SVK) constitutive model was used, with specific energy and second-order Piola-Kirchhoff stress (given by the concept of energy conjugate) evaluated as follows:

$$u_e(\mathbb{E}) = \frac{1}{2}\mathbb{E} : \mathbf{C} : \mathbb{E} \Rightarrow \mathbf{S} = \frac{\partial u_e}{\partial \mathbb{E}} = \mathbf{C} : \mathbb{E} \tag{4}$$

where $\mathbf{S}$ is the second-order Piola-Kirchhoff stress tensor, $\mathbb{E}$ is the Green strain tensor, and $\mathbf{C}$ is the fourth-order elasticity tensor.

Thus, the internal force vector presented in equation 1 results in:

$$F_i^{int} = \int_\Omega \mathbf{S} \frac{\partial \mathbb{E}}{\partial Y_i} d\Omega \tag{5}$$

2.1 Fibre coupling

To model the mechanical behaviour of fibres embedded in the solid, allowing the analysis of composite materials, the technique presented in Vanalli et al. [8] and extended by Sampaio et al. [9] for the position-based FEM approach has been used in this work. The technique does not add degrees of freedom to the problem and does not require the fibre nodes to coincide with the solid nodes. In addition, the version used in the present work considers perfect adhesion between the fibres and the matrix. The basic idea of the approach is to write the nodal positions of the fibres as a function of the nodal positions of the solids:

$$X_i^p = \phi_l(\xi_1^p, \xi_2^p) X_{li} \tag{6}$$

where ξ_1^p and ξ_2^p are the dimensionless coordinates of the fibre node defined in the solid domain (unknowns of the equation), ϕ_l are the solid shape functions (used in this study the bilinear quadrilateral element), X_{li} are the coordinates of the solid nodes in which the fibre node p of coordinates X_i^p is inserted and i and l are the indices denoting the direction and number of the solid node. The same equation is valid to determine the current positions of the fibre nodes Y_i^p.

As the dimensionless coordinates of the fibres in the solid domain are unknown, equation 6 is solved iteratively by the Newton-Raphson method. Thus, a tentative value is defined for the dimensionless coordinates of a given fibre node and the correction is calculated as:

$$X_i^p = \phi_l(\xi_1^{pt}, \xi_2^{pt}) X_{li} + \left.\frac{\partial \phi_l(\xi_1, \xi_2)}{\partial \xi_j}\right|_{(\xi_1^{pt}, \xi_2^{pt})} \Delta\xi_j \Rightarrow X_i^p - X_i^{pt} = H_{ij} \Delta\xi_j \tag{7}$$

where the subscript pt denotes the tentative value and $\Delta\xi_j$ is the correction of the dimensionless coordinates.

To represent the fibres, the present work adopts the simple bar element (truss). Once, the nodal position of the fibres in the solid domain is determined, the internal forces and tangent stiffness matrix of the fibres are calculated according to the truss element formulation [2] and this contribution is spread to the solid nodes. In the calculation of these contributions, the derivate of the strain energy in relation to the vector of current solid positions is performed. This derivate results in two terms: one associated to the solid contributions and another accounting to the fibre contribution multiplied by the solid shape function.

3 Extended Lumped Damage Mechanics

In LDM, and consequently in XLDM, it is assumed that inelastic effects are concentrated in regions with initially zero thickness, called localization bands, while the rest of the body remains elastic. From the work of Amorim et al. [24], the elongation equivalence hypothesis is proposed, inspired by the strain equivalence hypothesis presented in Lemaitre and Chaboche [27]. Thus, the deformed configuration of the solid elements is calculated from the elongations of virtual bar elements connecting the nodes. These considerations avoid mesh dependency problems arising from strain localization and often observed in classical damage mechanics formulations.

The proposal of Amorim et al. [24] is that five bars (called "numexes") are sufficient to describe the deformed behaviour along the finite element domain (Fig. 1). These numexes are allocated in a vector and calculated as:

$$\{\delta\} = [\mathbf{b}^Y]\{\mathbf{Y}\} - [\mathbf{b}^X]\{\mathbf{X}\} = \left\{\boldsymbol{\lambda}^Y\right\} - \left\{\boldsymbol{\lambda}^X\right\} \tag{8}$$

where $[\mathbf{b}^Y]$ and $[\mathbf{b}^X]$ are the matrices that transform nodal current and initial positions into elongations, defined generically as:

$$[\mathbf{b}] = \begin{bmatrix} -c_{ij} & -s_{ij} & c_{ij} & s_{ij} & 0 & 0 & 0 & 0 \\ -c_{ik} & -s_{ik} & 0 & 0 & c_{ik} & c_{ik} & 0 & 0 \\ -c_{il} & -s_{il} & 0 & 0 & 0 & 0 & c_{il} & s_{il} \\ 0 & 0 & -c_{jk} & -s_{jk} & c_{jk} & s_{jk} & 0 & 0 \\ 0 & 0 & 0 & 0 & c_{lk} & s_{lk} & -c_{lk} & -s_{lk} \end{bmatrix} \tag{9}$$

where c_{ij} and s_{ij} are the values of the cosine and sine of the angle formed by the segment ij with the horizontal axis, and so on. For the matrix $[\mathbf{b}^Y]$, the values are calculated from the current nodal positions and for the matrix $[\mathbf{b}^X]$ from the initial nodal positions.

This modelling assumptions allows the formulation to be geometrically exact, since the calculation performed from equation 8 results in the difference between the final and initial lengths of each numexe. Thus, the Green strain is calculated from the elongations of the previously defined numexes as:

$$\{\mathbb{E}\} = [\mathbf{T}^Y]\left\{\boldsymbol{\lambda}^Y\right\} - [\mathbf{T}^X]\left\{\boldsymbol{\lambda}^X\right\} \tag{10}$$

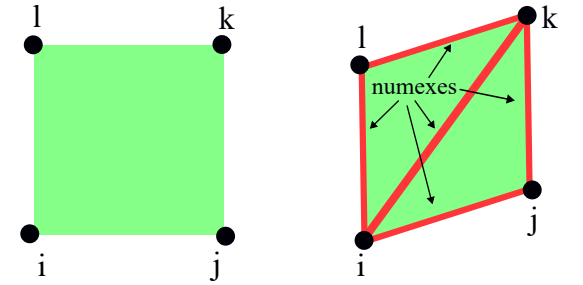

Figure 1. Finite element.

where the matrices $[\mathbf{T}^Y]$ and $[\mathbf{T}^X]$ are the transformation matrices, which involve the elongations of the numexes to the Green strain, calculated by:

$$\begin{aligned}[\mathbf{B}] &= [\mathbf{T}^Y][\mathbf{b}^Y] \\ [\mathbf{B}] &= [\mathbf{T}^X][\mathbf{b}^X]\end{aligned} \tag{11}$$

where $[\mathbf{B}]$ is the matrix that transforms displacements into Green strains. This matrix contains relations between the element shape functions derivatives.

Additionally, Amorim et al. [24] proposed the insertion of four localization bands on the element sides to compute the effects of material deterioration, while the element interior remains elastic (Fig. 2a). These localization bands have their growth controlled during the analysis from the verification of the damage laws:

$$g_i^{ij} = \sigma_i^{ij} - \sigma_{cr}\exp(qe_i^{ij}) \leq 0; \qquad g_j^{ij} = \sigma_j^{ij} - \sigma_{cr}\exp(qe_j^{ij}) \leq 0 \tag{12}$$

where σ_i^{ij} and σ_j^{ij} are the Cauchy stresses perpendicular to the band ij at nodes i and j, respectively e_i^{ij} and e_j^{ij}, σ_{cr} is the critical stress, and q is a material parameter, which describes the cohesive material characteristics (Fig. 2b). The same equation is used for the other localization bands.

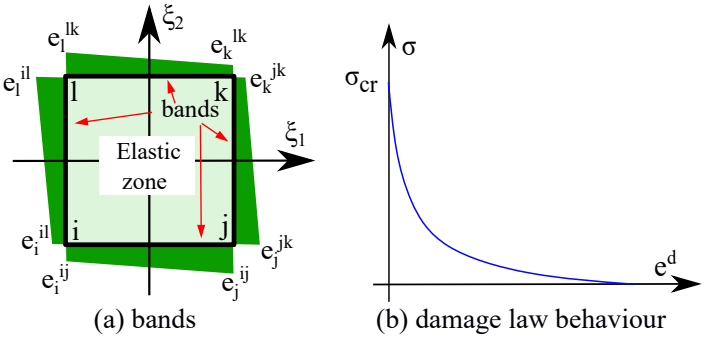

Figure 2. Localisation bands in XLDM element.

With the localization bands calculated, equation 13 is used to calculate the elongation of the numexes due to the material deterioration.

$$\left\{\boldsymbol{\delta}^d\right\} = [\mathbf{b}^Y] \begin{Bmatrix} s_{ij}e_i^{ij} - s_{il}e_i^{il} \\ -c_{ij}e_i^{ij} + c_{il}e_i^{il} \\ s_{ij}e_j^{ij} + s_{jk}e_j^{jk} \\ -c_{ij}e_j^{ij} - c_{jk}e_j^{jk} \\ s_{jk}e_k^{jk} - s_{lk}e_k^{lk} \\ -c_{jk}e_k^{jk} + c_{lk}e_k^{lk} \\ -s_{il}e_l^{il} - s_{lk}e_l^{lk} \\ c_{il}e_l^{il} + c_{lk}e_l^{lk} \end{Bmatrix} \tag{13}$$

Finally, using the SVK constitutive model and the Green strain components defined in this section, it is possible to calculate the second-order Piola-Kirchhoff stresses:

$$\mathbf{S} = \mathbf{C} : \left([\mathbf{T}^Y]\left\{\boldsymbol{\lambda}^Y\right\} - [\mathbf{T}^X]\left\{\boldsymbol{\lambda}^X\right\} - [\mathbf{T}^Y]\left\{\boldsymbol{\delta}^d\right\}\right) \tag{14}$$

4 Application

The accuracy and robustness of the numerical formulation proposed herein, based on the coupling of Extended Lumped Damage Mechanics and Finite Element Method based on positions with fibres, are verified in this application. The UHPRFC beam subjected to four-point bending tested by Lima et al. [28] is evaluated. Details of experimental geometry scheme is shown in Figure 3.

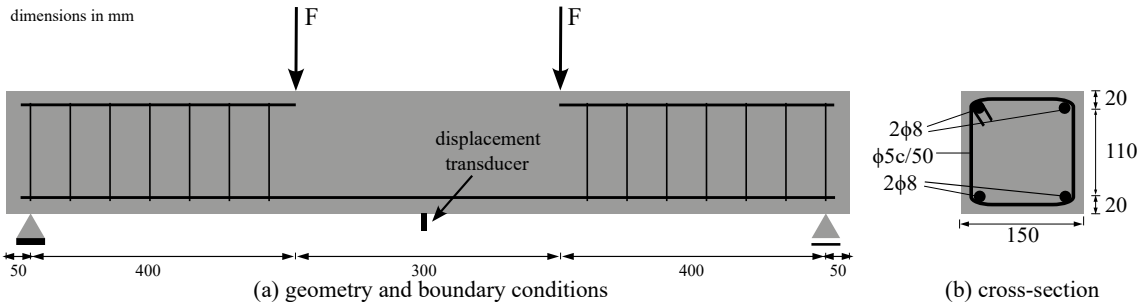

(a) geometry and boundary conditions (b) cross-section

Figure 3. Geometry and experimental data.

To model the beam presented in Figure 3, an elastic modulus of 15000 MPa, Poisson's ratio of 0.2, tensile strength of 6 MPa, and fracture energy of 0.40 N/mm have been adopted. Using equation 15 (presented in Teles et al. [26]), the value of $q = -15mm^{-1}$ is obtained. 2400 plane stress elements with thickness of 150 mm discretise the structure. The upper and lower longitudinal reinforcements have been discretised with bar elements of length 2.5 mm, resulting in 801 elements. The stirrups were discretized with a length of 2 mm, resulting in 784 elements. These reinforcements have been modelled assuming perfect plastic behaviour, with elastic modulus of 165 GPa and yield stress of 1000 MPa.

$$q = -\frac{f_t}{G_f}. \tag{15}$$

Figure 4 shows the comparison between the experimental and numerical responses obtained. It is observed that the proposed technique is able to reproduce the experimental behaviour of the UHPFRC beam subjected to four-point bending. In addition, it is noted that the obtained localisation bands show good agreement with those observed experimentally.

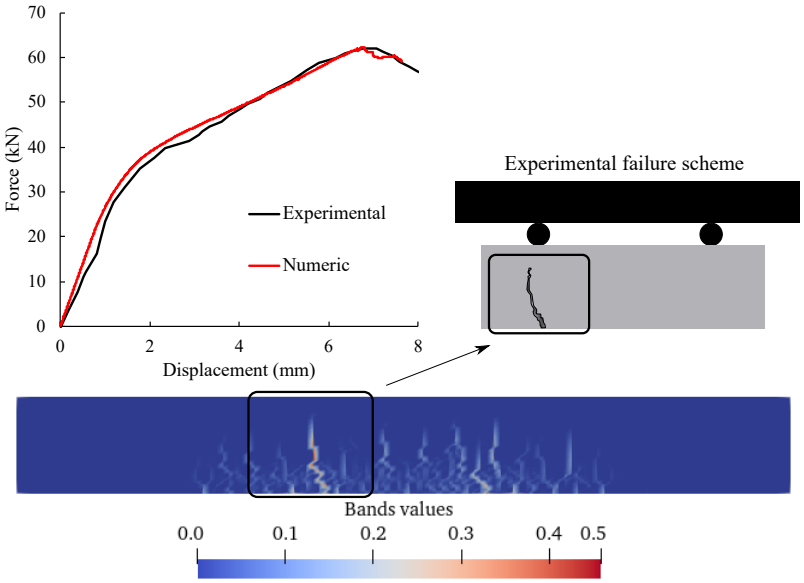

Figure 4. Results obtained.

5 Conclusions

In the present work, the failure of structures composed of UHPFRC was evaluated, considering the effects of material and geometric nonlinearities handled by XLDM and the FEM based on positions, respectively. The numerical tool was validated by the UHPFRC beam subjected to an experimental four-point bending test. The proposed technique was able to reproduce the experimental behaviour showing good agreement with the experimental results.

It is important to mention that the simulation was performed until some finite element reached the compressive strength of the concrete. This strategy has been adopted because the approach used in the present work does not consider compression degradation, which can be the subject of future work. In addition, the technique used to couple the fibres to the solid considers perfect adhesion, while in UHPFRC problems fibre slippage may occur. This is also a point that can be improved in future works.

Acknowledgements. The first author thanks the *Conselho Nacional de Desenvolvimento Científico e Tecnológico* (CNPq) for the financial support of his D.Sc. studies. The third author thanks the Fundação de Amparo à Pesquisa do Estado de São Paulo, project number 2022/03377-7, for the support.

Authorship statement. The authors hereby confirm that they are the sole liable persons responsible for the authorship of this work, and that all material that has been herein included as part of the present paper is either the property (and authorship) of the authors, or has the permission of the owners to be included here.

References

[1] H. B. Coda and M. Greco. A simple fem formulation for large deflection 2d frame analysis based on position description. *Computer Methods in Applied Mechanics and Engineering*, vol. 193, pp. 3541–3557, 2004.
[2] M. Greco, F. A. Gesualdo, W. S. Venturini, and H. B. Coda. Nonlinear positional formulation for space truss analysis. *Finite Elements in Analysis and Design*, vol. 42, pp. 1079–1086, 2006.
[3] H. B. Coda and R. R. Paccola. An alternative positional fem formulation for geometrically non-linear analysis of shells: Curved triangular isoparametric elements. *Computational Mechanics*, vol. 40, pp. 185–200, 2007.
[4] H. B. Coda, R. R. Paccola, and M. D. S. M. Sampaio. Positional description applied to the solution of geometrically non-linear plates and shells. *Finite Elements in Analysis and Design*, vol. 67, pp. 66–75, 2013.
[5] R. A. K. Sanches and H. B. Coda. On fluid–shell coupling using an arbitrary lagrangian–eulerian fluid solver coupled to a positional lagrangian shell solver. *Applied Mathematical Modelling*, vol. 38, pp. 3401–3418, 2014.
[6] J. P. Pascon and H. B. Coda. Finite deformation analysis of visco-hyperelastic materials via solid tetrahedral finite elements. *Finite Elements in Analysis and Design*, vol. 133, pp. 25–41, 2017.

[7] H. B. Soares, R. R. Paccola, and H. B. Coda. Unconstrained vector positional shell fem formulation applied to thin-walled members instability analysis. *Thin-Walled Structures*, vol. 136, pp. 246–257, 2019.
[8] L. Vanalli, R. R. Paccola, and H. B. Coda. A simple way to introduce fibers into fem models. *Communications in Numerical Methods in Engineering*, vol. 24, pp. 585–603, 2007.
[9] M. S. Sampaio, R. R. Paccola, and H. B. Coda. Fully adherent fiber–matrix fem formulation for geometrically nonlinear 2d solid analysis. *Finite Elements in Analysis and Design*, vol. 66, pp. 12–25, 2013.
[10] J. Flórez-López. Modelos de daño concentrados para la simulación numérica del colapso de pórticos planos. *Revista Internacional de Metodos Numericos para Calculo y Diseno en Ingenieria*, vol. 9, pp. 123–139, 1993.
[11] A. Cipollina, A. López-Inojosa, and J. Flórez-López. A simplified damage mechanics approach to nonlinear analysis of frames. *Computers & Structures*, vol. 54, 1995.
[12] M. E. Perdomo, A. Ramírez, and J. Flórez-López. Simulation of damage in rc frames with variable axial forces. *Earthquake Engineering & Structural Dynamics*, vol. 28, pp. 311–328, 1999.
[13] D. V. C. Teles, R. N. Cunha, D. L. N. F. Amorim, R. Picón, and J. Flórez-López. Parametric study of dynamic behaviour of rc dual system design with the brazilian standard code using the lumped damage model. *Journal of the Brazilian Society of Mechanical Sciences and Engineering*, vol. 43, pp. 246, 2021.
[14] D. L. N. F. Amorim, S. P. Proença, and J. Flórez-López. Simplified modeling of cracking in concrete: Application in tunnel linings. *Engineering Structures*, vol. 70, 2014.
[15] D. L. N. F. Amorim, S. P. B. Proença, and J. Flórez-López. A model of fracture in reinforced concrete arches based on lumped damage mechanics. *International Journal of Solids and Structures*, vol. 50, pp. 4070–4079, 2013.
[16] T. I. J. Brito, D. M. Santos, F. A. S. Santos, R. N. Cunha, and D. L. N. F. Amorim. On the lumped damage modelling of reinforced concrete beams and arches. *Frattura ed Integrità Strutturale*, vol. 14, pp. 1–20, 2020.
[17] Y. Bai, M. Kurata, J. Flórez-López, and M. Nakashima. Macromodeling of crack damage in steel beams subjected to nonstationary low cycle fatigue. *Journal of Structural Engineering*, vol. 142, pp. 04016076, 2016.
[18] Y. Bai, S. Guan, and J. Flórez-López. Development of a damage model for assessing fracture failure of steel beam-to-column connections subjected to extremely low-cycle fatigue. *Engineering Failure Analysis*, vol. 82, pp. 823–834, 2017.
[19] M. C. Oliveira, D. V. C. Teles, and D. L. N. F. Amorim. Shear behaviour of reinforced concrete beams under impact loads by the lumped damage framework. *Frattura ed Integrità Strutturale*, vol. 14, pp. 13–25, 2020.
[20] D. V. Teles, M. C. Oliveira, and D. L. Amorim. A simplified lumped damage model for reinforced concrete beams under impact loads. *Engineering Structures*, vol. 205, 2020.
[21] K. O. Coelho, E. D. Leonel, and J. Flórez-López. An efficient mechanical-probabilistic approach for the collapse modelling of rc structures. *Revista IBRACON de Estruturas e Materiais*, vol. 12, pp. 386–397, 2019.
[22] J. M. J. Oliveira, C. S. Vieira, M. F. A. Silva, and D. L. N. F. Amorim. Fracture modelling of steel fibre reinforced concrete structures by the lumped damage mechanics: Application in precast tunnel segments. *Engineering Structures*, vol. 278, pp. 115487, 2023.
[23] R. M. Bosse, J. Flórez-López, G. M. S. Gidrão, I. D. Rodrigues, and A. T. Beck. Collapse mechanisms and fragility curves based on lumped damage mechanics for rc frames subjected to earthquakes. *Engineering Structures*, vol. 311, pp. 118115, 2024.
[24] D. L. N. F. Amorim, D. Piedade Neto, S. P. Proença, and J. Flórez-López. The extended lumped damage mechanics: A new formulation for the analysis of softening with fe size-independence. *Mechanics Research Communications*, vol. 91, pp. 13–18, 2018.
[25] R. A. Picón, D. M. Santos, D. V. Teles, D. L. Amorim, X. Zhou, Y. Bai, S. P. Proença, and J. Flórez-López. Modeling of localization using nash variational formulations: The extended damage mechanics. *Engineering Fracture Mechanics*, vol. 258, pp. 108083, 2021.
[26] D. V. C. Teles, R. N. Cunha, R. A. Picón, D. L. N. F. Amorim, Y. Bai, S. P. B. Proença, and J. Flórez-López. A new formulation of cracking in concrete structures based on lumped damage mechanics. *Structural Engineering and Mechanics*, vol. 88, pp. 451–462, 2023.
[27] J. Lemaitre and J.-L. Chaboche. *Mécaniques des matériaux solides*, 1985.
[28] P. B. Lima, P. A. Krahl, F. A. Silva, and D. C. T. Cardoso. A modeling strategy for the flexural performance prediction of uhpc beams accounting for variability of properties. *Composite Structures*, vol. 322, pp. 117374, 2023.